AN INVESTIGATION ON THE TIMING OF FORMATION OF THE WRINKLE RIDGES ON THE LUNAE PLANUM AND ON THE SYRTIS MAJOR PLANUM. T. Ruj[1] and K. Kawai[1], [1]Department of Earth and Planetary Science, School of Science, University of Tokyo, Hongo 7-3-1, Bunkyo, Tokyo 113-0033, Japan. (trishit@eps.s.u-tokyo.ac.jp).

Introduction: The compressional structures are widely distributed on the surface of Mars. Wrinkle ridges (WR) are the most common amongst them [1, 2]. These linear ridges are distributed on the surface of possible volcanic origin [1, 3] and runs over 1000 km in length with highest width of 10-15 km. However, there are instances where WRs are observed on the impact basin floors following the curvature of the outer arc of the basin rim (e.g., Huygens Crater on the southern highlands). WRs are also common on the floors of the large impact basins with no preferable orientations (e.g. Hellas, Isidis), as well as in the surroundings of the volcanic patera regions [4, 5]. In addition, the study of the morphometry of the WRs can strengthen our knowledge on the understandings of the operated paleostress activities operated on the Martian surface. Therefore, the global distribution of the WRs and their estimated ages could be beneficial towards the development on understandings of the early evolution of the red planet. However, in a broader perspective such understandings might help us to know our own planet better, as most of the early remnants of crustal activities were destroyed by the intense geological processes.

Here, in this abstract we report on our preliminary investigation conducted for the age estimation of WR distribution using Buffer Crater Counting (BCC) from the Lunae Planum and Syrtis Major Planum.

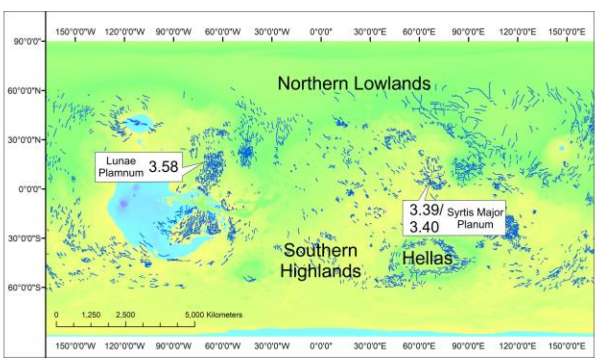

Figure 1. Figure showing the distribution of the contractional features on the Martian surface. White boxes indicate the age (in Ga) of the Lunae Planum (3.58 Ga) and Syrtis Major Planum (3.39/3.40 Ga).

Materials and Method: We primarily identified the WRs using the global maps of the linear surface tectonic features of Mars [6, 7] overlying the Thermal Emission Imaging System (THEMIS)-InfraRed (IR) day time [8] Global Mosaic and Mars Orbital Laser Altimeter (MOLA) [9] colorized elevation maps. Then, we used available global [10] and local scale maps [11-14] to reinvestigate each characteristic structures using high resolution Context (CTX) camera images (6 m/pixel) [15] and High-Resolution Stereo Camera (HRSC)-MOLA blended Digital Elevation Models (DEM) (200 m/pixel) [16]. These images and DEMs helped us to discriminate WRs from other linear structures (e.g., lobate scarp, ridge) of compressional/contractional origin. We used CraterTools (an ArcGIS add on [17]) for digitization and crater counting. Counted craters were statistically analyzed using Craterstats II [18].

We applied the BCC method [19], following the strategies of Kneissl et al. (2015) [20]. BCC method is a modified version of Crater Size frequency Distribution (CSFD) which allows a direct estimation of the ages of the WRs on Mars. Earlier, Mangold et al. (2000) [21] estimated the ages of the compressional deformational structures on the surface of Mars using low-resolution Viking images. However, here in this investigation, we used high-resolution CTX images to estimate the age of WR association characterized by orientations, morphology and the nature of the basement. We have successfully derived absolute model ages (in terms of number) for each set of WRs instead of a wide time frame which is usually used in absence of boundary defining geologic phenomenon.

For the BCC procedure we included the craters that are in direct contact with the WRs, which includes the wrinkled part on the top of the ridge and leading and trailing the associated faults. We had to exclude craters from the hump of the WRs (if it is not associated with the crenulated part on the top or any other associated linear components developed during the time of the ridge growth) due to the uncertainty related to the subsequent upliftment of the craters.

Geological Background of WRs: WRs have two main morphological elements, a broad ridge and a sinuous and crenulated part on the top of the ridge [3, 22, 23]. This crenulated part is named as wrinkle. However, the mechanism related to the origin of these WRs has been a topic of discussion among the scientists for decades. Explanations include thrust that leads to buckle folding [3]; shortening of the rigid upper volcanic rock-rich crustal blocks (due to thrust faulting) with indefinite depth extent of the associated thrust fault [24, 25]; association with two thrust faults that dip oppositely [26]; fault bended fold [27]; relation to fault propagation fold [28]; association with sub-surface thrust faults, and folding of near-surface basement layers [29].

Distribution of Winkle Ridges: The WRs are well distributed almost throughout the entire Mars with multiple orientations. Morphology of the WRs also differ with the variations in the stress pattern and the thickness of the layered basement rock [1]. Multiple and crosscutting relationships with random orientations of the WRs imply isotropic stress pattern operating at a similar time within a single terrain.

Here, in this abstract we have opted to estimate the age of two different terrains (Figure 1). First one is the WRs of Lunae Planum and the second one is the WRs of the Syrtis Major Planum. The WRs in the Lunae Planum are regularly spaced with almost constant North-South strike. On the other hand, WRs in the Syrtis Major Planum are in concentric and radial orientations around the central caldera [30].

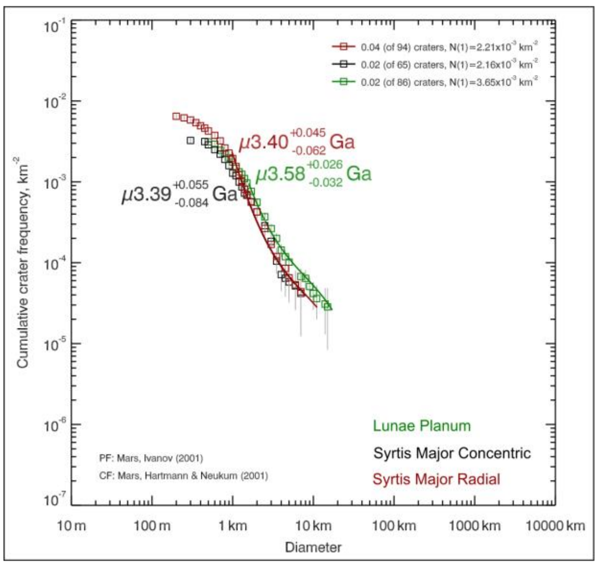

Figure 2. Estimated Absolute Model Ages (AMA) for the WRs in the Lunae Planum (marked in green) is 3.58 Ga. This age corresponds to the global contractional period of the early Hesperian Period [31]. The AMAs for the concentric (black) and radial (red) WRs of the Syrtis Major Planum are 3.39 and 3.40 Ga respectively.

Age of Wrinkle Ridges: Most of the Martian WRs are formed around the early to late Hesperian [21]. We have mapped the WRs of the Lunae Planum of a cumulative length over 22,000 km. We have analyzed more than 500 craters (from ~300 m to 22 km) to estimate the age. The BCC derived age indicates that the WRs of Lunae Planum is $3.58^{+0.026}/_{-0.032}$ Ga (Figure 2) old. The Crater retention age N(1) is 3.65×10^{-3} km^{-2} and 86 craters of 1.6 to 17 km diameter were fitted to estimate the age.

Concentric WRs in the Syrtis Major Planum of a total length of more than 10000 km were mapped. We have estimated the age of $3.39\ ^{+0.055}/_{-0.084}$ Ga (Figure 2) analyzing around 170 craters from ~150 m to 7.75 km diameter. The crater retention age N(1) is 2.16×10^{-3} km^{-2} and 65 craters from 1.23 to 8 km diameter were fitted to extract the age.

To estimate the age of the radial WRs in the Syrtis Major Planum, we have mapped over 9000 km and considered over 260 craters from ~240 m to ~15 km diameter. The extracted age is $3.40^{+0.045}/_{-0.062}$ Ga (Figure 2) considering 94 craters of 990 m to 11 km in diameter. The crater retention age N(1) is 2.21×10^{-3} km^{-2}.

Conclusion: In an intension to extract the WRs of Mars on a global scale to understand the early Martian evolution, we have found that there was a dominant compressional stress around 3.58 Ga, in and around the Tharsis region. This timing also corresponds to the global contractional period of Mars. However, the estimated age and the orientations of the WRs in the Syrtis Major Planum tells about the timing of the volcanic activity of the region.

Acknowledgments: This work was supported by JSPS KAKENHI Grant Number 18F18312 to TR and KK. We acknowledge NASA's Planetary Data System and Murrey Lab for CTX data and their mosaic.

References: [1] Watters T. R. (1993) *JGR: Planets, 98(E9),* 17049–17060. [2] Mueller K. and Golombek M. (2004) *Annu. Rev. Earth Planet. Sci., 32,* 435–464. [3] Watters T. R. (1988) *JGR: Solid Earth, 93(B9),* 10236–10254. [4] Mangold N. et al. (2002) *Planet. Space Sci., 50(4),* 385–401. [5] Williams D. A. et al. (2010) *Earth Planet. Sci. Lett., 294(3-4),* 492–505. [6] Knapmeyer M. et al. (2006) *JGR: Planets, 111*(E11). [7] Knapmeyer, M. et al. (2008) *EGU X,* Abstract # A-03574. [8] Christensen P. R. et al. (2004) *Space Sci. Rev., 110(1–2),* 85–130. [9] Smith M. D. et al. (2001) *GRL, 28(22),* 4263–4266. [10] Tanaka K. L. et al. (2014) *Planet. Space Sci., 95,* 11–24. [11] Tanaka, K.L. et al. (2005) *USGS,* 1–27. [12] Bernhardt H. et al. (2016) *Icarus, 264,* 407–442. [13] Leonard G. J. and Tanaka K. L. (2001) *USGS,* 1–10. [14] Ruj T. et al. (2017) *J. Maps, 13(2),* 755–766. [15] Malin M. C. et al. (2007) *JGR: Planets, 112(E5).* [16] Fergason R. L. et al. (2018) *USGS,* http://bit. ly/HRSC_MOLA_Blend_v0. [17] Kneissl T. et al. (2011) *Planet. Space Sci., 59(11-12),* 1243–1254. [18] Michael G. G. and Neukum G. (2010) *Earth Planet. Sci. Lett., 294(3-4),* 223–229. [19] Fassett C. I. and Head III J. W. (2008) *Icarus, 195(1),* 61–89. [20] Kneissl T. et al. (2015) *Icarus, 250,* 384–394. [21] Mangold N. et al. (2000). *Planet. Space Sci., 48(12-14),* 1201–1211. [22] Maxwell T. A. et al. (1975) *Geol. Soc. Am. Bull., 86(9),* 1273–1278. [23] Sharpton V. L. and Head J. W. (1988). *LPS XVIII,* 307–317). [24] Plescia J. B. and Golombek M. P. (1986) *Geol. Soc. Am. Bull., 97(11),* 1289–1299. [25] Plescia J. B. (1991) *JGR: Planets, 96(E3),* 18883–18895. [26] Allemand P. and Thomas P. (1992). *Academie des Sciences Paris Comptes Rendus Serie B Sciences Physiques, 315,* 1397–1402. [27] Suppe J. and Connors C. (1992). *JGR: Planets, 97(E8),* 13545–13561. [28] Mercier E. et al. (1997). *J. Struct. Geol., 19(2),* 185–193. [29] Schultz R. A. (2000) *JGR: Planets, 105(E5),* 12035–12052. [30] Hiesinger H. and Head III J. W. (2004). *JGR: Planets, 109*(E1). [31] Ruj T. et al. (2019) *Geosci. Front., 10(3),* 1029–1037.